# 自適應式液體探頭的開發與其在阻抗式齲齒檢測系統的應用

## A Self-Adaptive Fluidic Probe for Electrical Caries Detection

利用液體探頭可隨牙齒形貌改變形狀的特性，並以氣流控制探頭與牙齒的接觸範圍及隔絕環境干擾，與受測牙齒建立密合連結並測量其穿透阻抗；實驗證明牙齒阻抗與齲齒程度大致成反比，利用液體探頭可有效測得齲齒所造成>20倍的阻抗變化，並能滲入難以探測的牙縫搜尋鄰接面齲齒，早期發現並控制齲齒的危害。

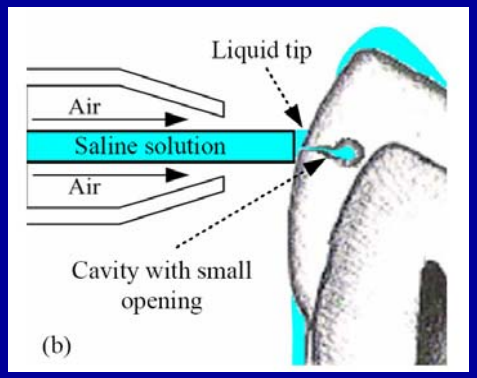


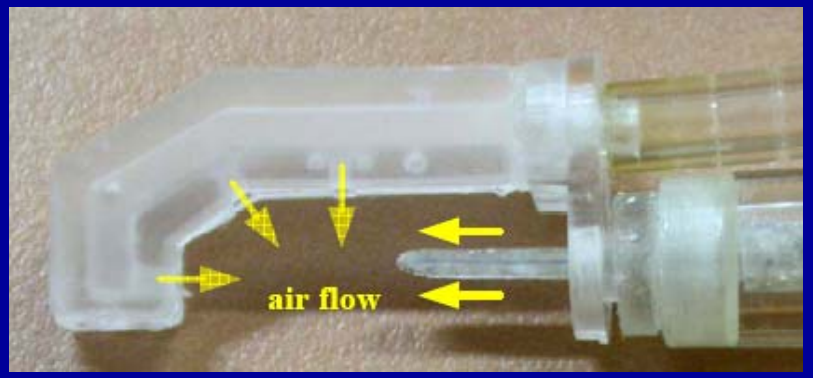


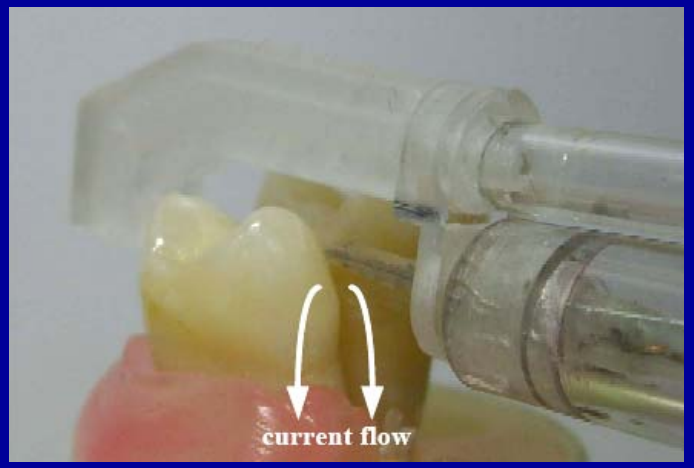

Biomed Microdevices (2008) 10:447–457
DOI 10.1007/s10544-007-9154-3

# A self-adaptive fluidic probe for electrical caries detection

**Shao-Hsuan Chang · Yu-Chuan Su**

Published online: 17 January 2008


**Abstract** This paper presents a miniature fluidic probe that is capable of self-adapting its shape to teeth and cooperating with electrical devices to detect dental caries by sensing the variation in electrical- impedance. The fluidic probe, whose liquid tip spontaneously spreads on hydrophilic tooth surface and into underlying caries, is employed to create intimate electrical contact for impedance sensing. A tubular air sleeve shaped by the probe casing is applied around the liquid tip to insulate it from surrounding saliva, and to regulate its spreading. In addition, a friction damper is integrated to stabilize the actuation of fluidic probe. In the prototype demonstration, un-restored, extracted premolar teeth were investigated and the results indicated >20-fold impedance differences between sound and carious teeth, by which caries could be identified in a consistent manner. Furthermore, the fluidic probe has been applied to detect approximal caries, which locates in the contacting surfaces of two adjacent teeth and is difficult to detect by most available schemes. As such, the proposed self-adaptive fluidic probe could readily serve as a diagnostic tool, which is critical to caries prevention and various dental-care applications.

**Keywords** Caries detection · Capillarity · Impedance sensing · Fluidic probe · Surface tension

## 1 Introduction

Dental caries, also described as tooth decay, is an infectious microbiological disease that causes localized dissolution and destruction of teeth (Sturdevant et al. 1985). In general, teeth are undergoing a dynamic process involving back-and-forth de-mineralization and re-mineralization. Tooth decay is mainly caused by certain types of bacteria that consume fermentable carbohydrates and produce organic acids on tooth surfaces. Locally, the produced organic acids significantly accelerate the de-mineralization process and eventually result in permanent tooth decay, if the destruction is too severe to be recovered by natural re-mineralization. Allowing dental caries to proceed untreated might subsequently result in the infection of dental pulp, which could cause suffering, tooth loss, advancing infection, and in the most severe (but rare) cases, death. It is one of the world's most common chronic diseases with an estimated 60–90% of school-children and the vast majority of adults having experienced dental caries (Peterson 2003). Considering the enormous costs (including direct restoration expenses and indirect/intangible ones) caused by dental caries, the management of dental caries is critical to our society and deserves serious public attention.

Modern management of dental caries, which includes prevention, control, and treatment, is based on the diagnosis of the disease and the detection of its pathological changes (Tranæus et al. 2005). Conventionally, caries diagnosis relies on visual observation of texture and discoloration, clinical judgment based upon experience, and on tactile sense by probing with an explorer. In addition, bitewing radiography could be employed to reveal the internal structures of teeth and assist the identification of caries. However, it is found that only a limited portion of the caries present could be detected using conventional clinical and radiographic methods (Selwitz et al. 2007). With modern technology, early caries detection is feasible and critical for conducting timely and appropriate preventive measures (Pretty 2006). Previously, researchers have demonstrated caries detection by various optical (Keem and Elbaum 1997), ultrasonic (Lees and Barber 1968; Culjat et al.

S.-H. Chang · Y.-C. Su (✉)
Department of Engineering and System Science,
National Tsing Hua University,
101, Section 2, Kuang-Fu Road,
Hsinchu, Taiwan
e-mail: ycsu@ess.nthu.edu.tw

2003), fluorescent (Benedict 1929; Sundström et al. 1985; Hibst and Gall 1998), and electrical (Mumford 1956; White et al. 1978; Longbottom et al. 1996) schemes. Among these schemes, electrical sensing is the most promising one for home-care applications because of its simplicity, low cost, and potentially high sensitivity. With affordable prices and simple operation, regular caries checks performed by parents or school teachers could potentially be realized. In the early investigations of electrical caries detection, continuous (Mumford 1956) and low-frequency alternating currents (White et al. 1978) were employed to measure the resistances or impedances of teeth. Aiming to collect more detailed characteristics of teeth, electrical impedance spectroscopy (EIS), which scans over a wide range of frequency (Kumasaki 1975; Levinkind et al. 1990; Barsoukov and Macdonald 2005), has replaced the fixed-frequency methods for electrical caries detection in recent years (Longbottom et al. 1996; Huysmans et al. 1996). Probes with various geometries and materials, for example a sharp metal tip with or without an air-flow (Ashley et al. 1998; Longbottom and Huysmans 2004), a carbonated fiber (Huysmans et al. 1996), and a metal-coated plastic strip or wedge (Longbottom et al. 1993) have been employed to establish intimate electrical contact between tooth sample and impedance-sensing device. Unfortunately, the imperfect probe-to-tooth contact and the disturbances from surrounding saliva usually lead to significant measurement errors and hinder the application.

To eliminate these deviations and to achieve consistent electrical caries detection, a new scheme is therefore developed. This work presents a new scanning probe that is capable of self-regulating the electrical contact to achieve reliable impedance sensing. Three accomplishments have been achieved: (1) the employment of a miniature liquid tip that can create intimate and penetrating electrical contact; (2) the application of a shielding air-flow that insulates the liquid tip from surrounding saliva; and (3) the development of a consistent detection scheme that can even be applied to detect approximal caries, which is barely sensed by existing techniques. As such, the proposed self-adaptive fluidic probe could readily serve as a safe and low-cost diagnostic tool, which is critical to caries prevention and dental-care applications.

## 2 Operation principle

### 2.1 Electrical caries detection

Ideally, the detection is based on the fact that sound dental hard tissues show extremely high impedances, while de-mineralized tissues become porous and filled with surrounding fluids, which results in much lower impedances. A sound tooth consists of four major tissues: enamel, dentin, pulp and cementum, as illustrated in Fig. 1. Among these tissues, the outermost, enamel is composed of tightly packed hydroxyapatite crystallites, which have extremely high impedance. Early in its development, caries may affect only enamel, which loses minerals and becomes porous as it undergoes demineralization. This porosity is filled with ion-rich fluids from the oral environment. Increased ionic content in these pores leads to increased electrical conductivity, or, conversely, increased porosity leads to decreased electrical impedance. Once enamel has been lost locally and the extent of decay reaches dentin, the considerable movement of ions through damaged enamel can result in the acid dissolution of dentin before the cavitation on enamel surface. Dentin is a porous yellow-hued material, which contains many fluid-filled tubules and therefore has a relatively low electrical impedance. Since dentin decays more rapidly than enamel, in many cases severe decay exists while showing relatively little sign on tooth surface. The conductivity increases dramatically when the de-mineralization reaches dentin.

To sense the impedance (and structural) variation caused by dental caries, a conducting path from tooth surface to root is created (as illustrated in Fig. 2) by placing a point contact on the surface. The conduction of current through a tooth, which can be modeled as capacitors and resistors connected partially in parallel and partially in series (with ignorable inductance effects) (Longbottom et al. 1996; Levinkind et al. 1990; Huysmans et al. 1996), is also illustrated in the figure. As explained by the model, electrical impedance measurement is hampered by polarization when direct or low-frequency alternating currents are employed. Usually the measurement is performed at a fixed frequency, while a scanning over a wider range of frequency (or electrical impedance spectroscopy, EIS) can be employed to determine more detailed information about the electrical characteristics of teeth. To account for the non-homogeneous distribution of capacitors and resistors

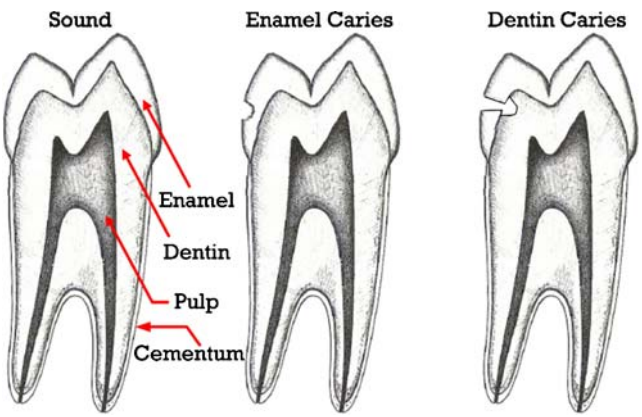


**Fig. 1** Cross-sectional views of sound, enamel carious, and dentin carious premolar teeth

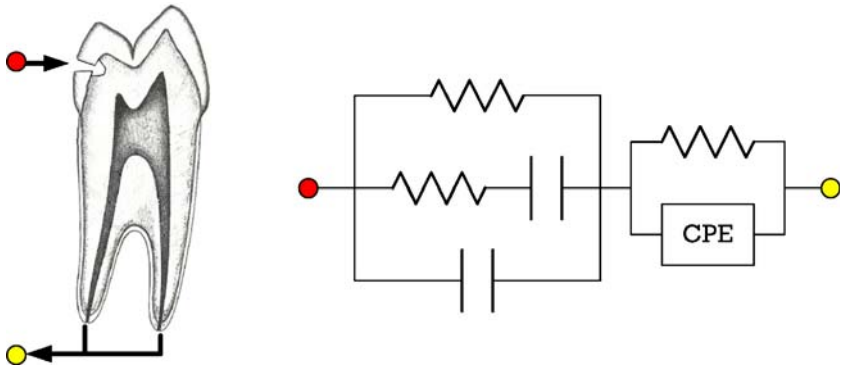


**Fig. 2** Schematic of the conducting path through a tooth and its equivalent circuit

inside a tooth, a constant phase element (CPE) is also included in the model.

## 2.2 Fluidic probe

To establish intimate electrical contact between tooth sample and impedance-sensing device, probes with various geometries and materials have been employed. A sharp probe usually has high spatial resolution, but the resulting contact resistance is high and the time required to scan over the entire surface of a tooth is long. To achieve high sensitivity, large sensing area (therefore short scanning time), and low contact resistance at the same time, a fluidic probe with liquid tip and shielding air sleeve has been developed and its working principle is illustrated in Fig. 3. The liquid tip is actually a saline solution continuously supplied from an upstream reservoir. It is preferred to have the liquid tip self-regulated, so that its shape and volume can be self-adapting to the tested sample through the scanning process. Since the outermost enamel layer of a tooth is hydrophilic, the aqueous tip spontaneously spreads on the tooth surface once a contact is made. The liquid tip deforms correspondently to the terrain and establishes a conformal contact with low impedance. In addition, capillary forces will drive the saline solution penetrating into caries with extremely small porosity, which can hardly be detected by conventional solid probes. Furthermore, the liquid tip is shielded by a tubular air sleeve, which insulates the tip from the thin saliva film distributed around the contact point. Otherwise, the highly conductive saliva film may create extra conducting paths, which usually result in false low impedance readings.

The liquid tip experiences four different types of forces, resulting from: gravity, surface tension, air pressure, and friction. A highly viscous fluid, which functions as a damper, is filled on top of the saline solution to provide the friction acting against any relative motion between the filled fluids and the probe. Among these forces, air pressure and friction are introduced to act against gravity and surface tension, and to achieve the desired self regulation as illustrated in Fig. 4. According to Young-Laplace equation (Adamson and Gast 1997),

$$(\Delta P)_e = \gamma\left(\frac{1}{r_1}+\frac{1}{r_2}\right), \tag{1}$$

the pressure difference across an equilibrium interface, $(\Delta P)_e$, can be determined by the geometries ($r_1$ and $r_2$ are the radii of curvature) and tension ($\gamma$) of the interface. On the other hand, the actual pressure difference across the interface ($\Delta P$) is

$$\Delta P = P_{air} - P_g + P_f, \tag{2}$$

where $P_{air}$, $P_g$, and $P_f$ are the pressures resulted from airflow, gravity, and friction, respectively. Considering the

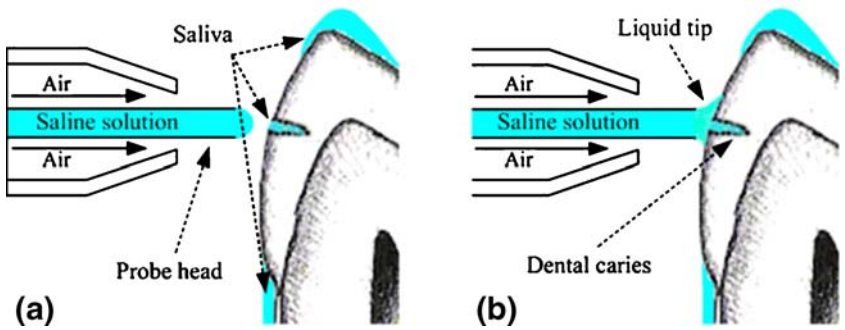


**Fig. 3** (**a**, **b**) Schematic of the presented detecting principle

situation illustrated in Fig. 4(a), $r_1$, $r_2$, and $(\Delta P)_e$ are estimated to be

$$r_1 = r_2 = \frac{R}{\cos\theta} \text{ and } (\Delta P)_e = \frac{2\gamma}{r_1} = \frac{2\gamma}{R}\cos\theta, \quad (3)$$

where $R$ is the radius of the probe and $\theta$ is the contact angle of water on the hydrophobic probe surface. In this case, the frictional force resulting from the highly viscous fluid can potentially cancel out the gravity forces applying on the saline solution and prevent it from dripping out of the probe. Once a contact is made, the interfacial tension will drive the saline solution to spread on the hydrophilic tooth surface. Considering the situation shown in Fig. 4(b), $r_1$, $r_2$, and $(\Delta P)_e$ are estimated to be

$$r_1 = \frac{d}{\cos\psi + \cos\theta} \text{ and}$$
$$(\Delta P)_e = \gamma\left(\frac{1}{r_1} + \frac{1}{r_2}\right) = \gamma\left(\frac{\cos\psi + \cos\theta}{d} - \frac{1}{R}\right) \quad (4)$$

where $d$ is the distance between the probe and the tooth surface, and $\psi$ is the contact angle of water on the hydrophilic tooth surface. Figure 5 illustrates the relationship between the pressure (and pressure differences) involved in the self-regulation mechanism when the probe-to-surface distance ($d$) varies. The values are estimated based on the conditions that a 3-cm-long jelly column, which has a dynamic frictional pressure of 800 Pa, is applied on top of a 10-cm-long saline column, which also experiences a constant air pressure of 1,400 Pa on its bottom sidewall. The contact angles on the probe and tooth surfaces are assumed to be 100° and 25°, respectively. It is noticed that capillary force dominates in the range of d <35 μm, with high $(\Delta P)_e$ values beyond what $\Delta P$ can potentially reach. As such, it results in the continuous spreading of saline solution on tooth surface. On the other hand, the varying $P_f$ is the critical component that accomplishes the self-regulation of liquid tip. To maintain the liquid tip in equilibrium, the actual value of $P_f$ is self-adjusted by

$$P_f = (\Delta P)_e - P_{air} + P_g \quad (5)$$

It either acts with $P_{air}$ to stop further spreading, or acts against $P_{air}$ to prevent back-flowing. Finally, when the liquid tip is moving away from the tooth surface, it eventually breaks into two parts with one remains on the tip and the other one left on the tooth surface.

## 3 Fabrication processes

Figure 6 illustrates the detailed assembly diagram of the proposed fluidic probe. The cross-shaped probe head functions as a supporting structure to guide the fluid and current flows. Meanwhile, pressurized air flows through the holes on the flow guide, nozzle, and finally forms a tubular air sleeve around the probe tip. The probe head was fabricated by a laser micromachining process. First of all, a 300-μm-wide and 200-μm-deep groove was shaped on a 1-mm-thick poly-methylmethacrylate (PMMA) substrate (ACRYREX, Chi Mei) using a $CO_2$ laser machine (Laser-Pro Venus, GCC) set at a laser power of 1 W and a scanning rate of 0.2 m/s. To reduce the unwanted conducting resistance, the sidewalls of the groove, which would be filled with saline solution, were then coated with conducting silver paste (RF1008A, Hong How Technology) by screen printing. Furthermore, the inner space of the groove was shaped by a molding process, and the extra paste spilled on the substrate was then removed right away to keep the surface flat and clean. Afterward, the substrate was baked for

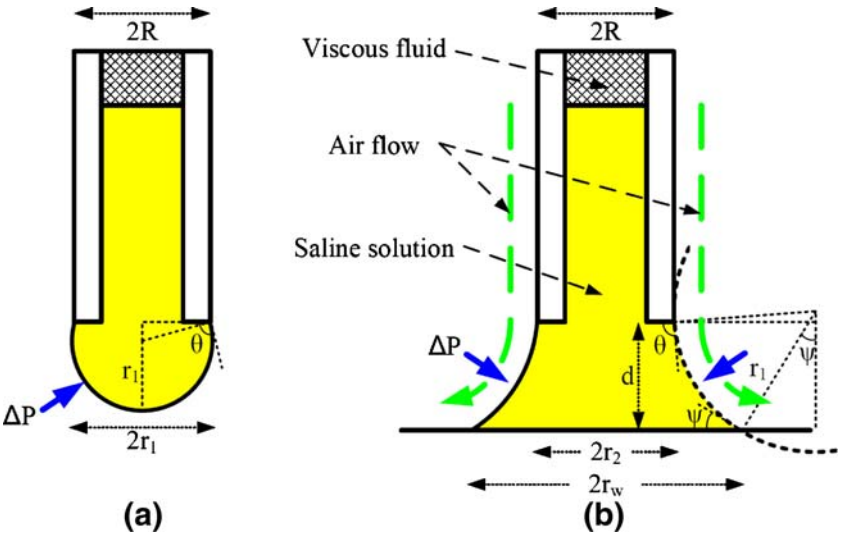


**Fig. 4** (**a**, **b**) Schematic of the self-regulation mechanisms

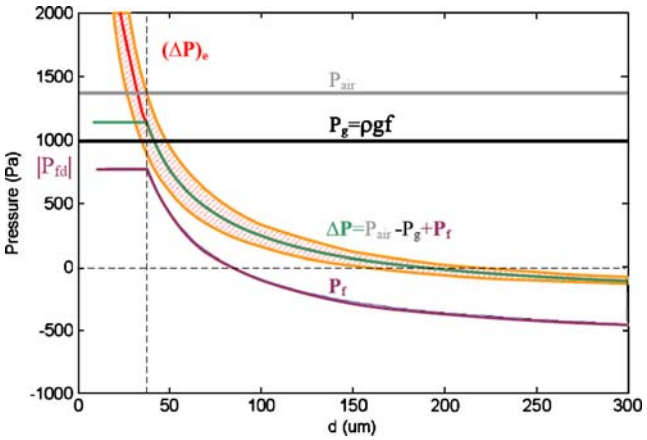


**Fig. 5** Relationship between the pressures (and pressure differences) involved in the self-regulation mechanism when the probe-to-surface distance (*d*) varies

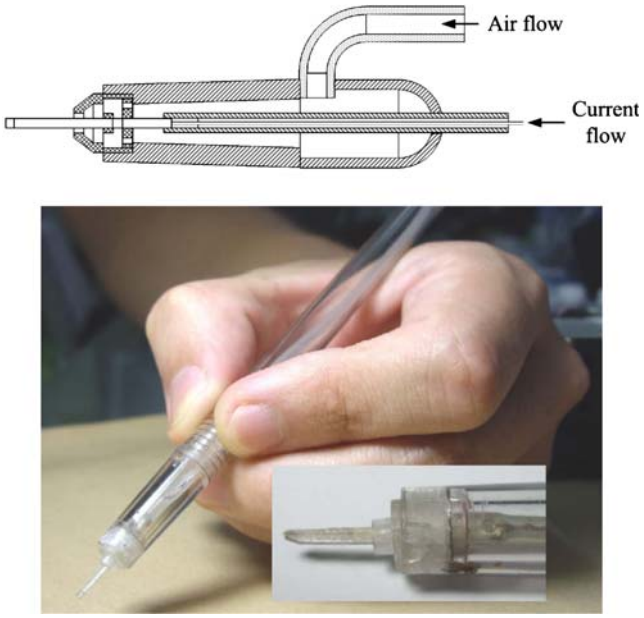


**Fig. 7** Cross-sectional view and photograph of a fabricated probe

30 min to solidify the conducting coating. To seal the groove, a 50-μm-thick polyester sheet coated with EVA-based hot melt adhesive (Loctite Hysol 1942) was laminated on top of the substrate. The polyester sheet was rolled (with a constant velocity of 1 mm/s) and pressed by a hot laminator (1 MPa at 140°C) to seal the groove. Finally, the cross-shape probe head was split from the substrate using the laser machine set at its maximum power output. Meanwhile, the nozzle, holder, and guide were all fabricated using a micro milling machine (MDX-15, Roland) with a 300-μm-in-diameter tool. These structures were also machined from PMMA substrates with thicknesses ranging from 1 to 3 mm. The nozzle and holder are 5 mm in outer diameter, and tightly assembled into the probe housing as illustrated in Fig. 6. The cross-sectional view and photograph of the whole fabricated probe are shown in Fig. 7.

## 4 Experimental details

Prior to the caries detection trials, the regulated wetting of the proposed liquid tip on a hydrophilic surface was first characterized. It was measured that a minimum pressure difference of 890 Pa is required to drive a 3-cm-long K-Y Jelly segment to move inside a silicone tube of 500 μm in inner-diameter. Based on our estimation, the frictional force provided by this jelly segment is sufficient to hold a 10-cm-long saline column against the gravity. Prototype probes with a liquid tip of roughly 500 μm in diameter were mounted on a xyz stage and slowly brought into contact with a glass slide. The slide surface is hydrophilic and has a contact angle of roughly 25°, which is close to that of tooth surface. Once the liquid tip touched the surface, the resulted capillary force tended to draw liquid out of the probe. Figure 8 shows the profiles of two liquid tips operated under different air pressures ($P_{air}$=500 or 1,400 Pa) and at various probe positions ($d$=100, 200, or 300 μm). With $P_{air}$=500 Pa and $d$=100 μm, the air pressure was found to be too low to stop the outgoing spreading. An excessive amount of liquid wetted on the outer sidewall of the probe and eventually the movement stopped as illustrated in the figure. The profile in this case is very similar to the one under the conditions of $P_{air}$=500 Pa and $d$=200 μm, in which an equilibrium was reached in the gap. Further movement to $d$=300 μm eventually broke the liquid tip

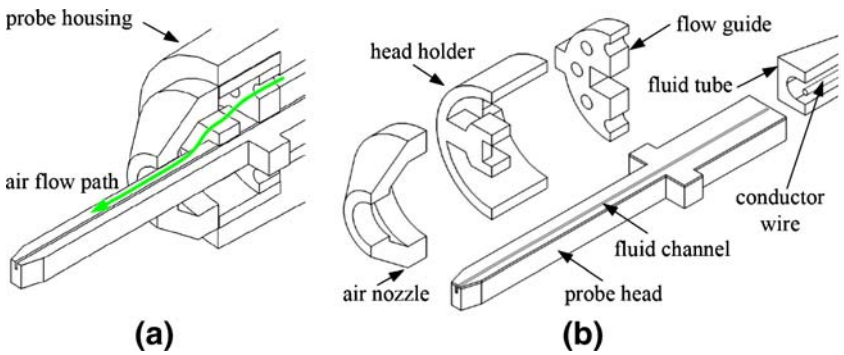


**Fig. 6** (**a**, **b**) Assembly diagram of the proposed fluidic probe

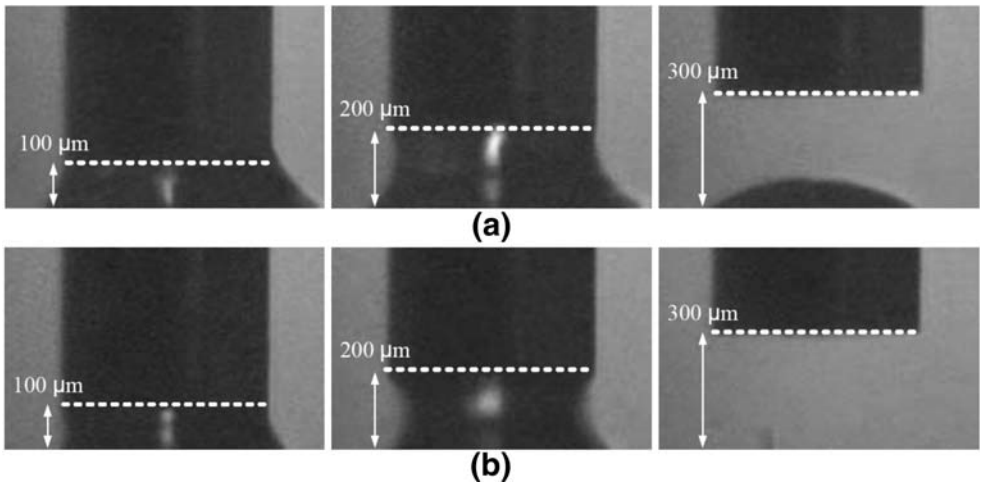


**Fig. 8** Profiles of two liquid tips at various probe positions while air pressures of (**a**) 500 Pa and (**b**) 1,400 Pa were applied

with one part remained on the surface. On the other hand, with $P_{air}$=1,400 Pa, the liquid tip was confined in the gap and the resulted contact area was relatively smaller. When in equilibrium, the radius of the contact area can be estimated as:

$$r_w = R + r_1(\sin\theta - \sin\psi), \tag{6}$$

in which all the symbols were defined as illustrated in Fig. 4. The electrical impedance of the probe itself was measured and the result (with $d$=100 μm) is illustrated in Fig. 9. Over the measured frequency range, the probe behaved like a resistive component and showed a constant impedance of roughly 55 Ω, which is several orders smaller in magnitude than those of carious teeth. When moving the probe away from the contact, the measured impedance varied but remained less than 100 Ω before the liquid tip was finally broken. While connected in series with tooth samples, the probe would contribute only a negligible portion of the resulting total impedance.

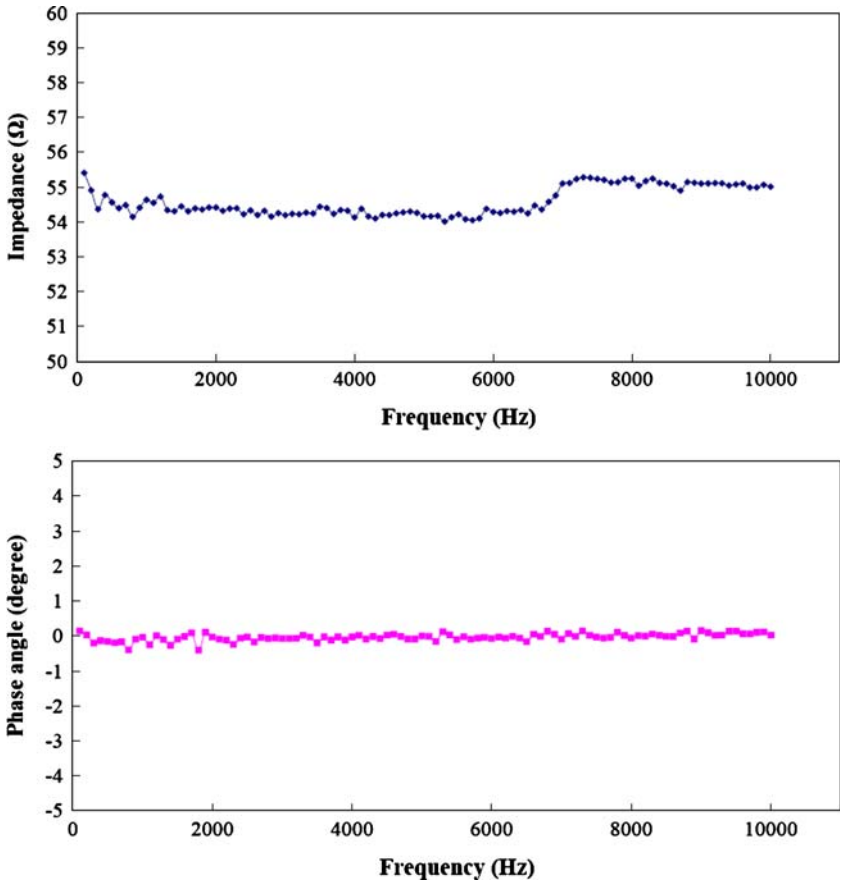


**Fig. 9** Electrical impedance of the proposed fluidic probe

In this work, all tested samples were un-restored, extracted premolar teeth, which showed no signs of non-carious damage such as fractures or abrasions on their surfaces. The samples were dried for 30 s with compressed air and examined under a standard dental operating light by a certified dentist using a dental explorer. The identification of sound and potential carious sites basically followed the criteria developed by Downer (Downer 1975), while the samples were classified as sound, enamel, and dentin carious. Overall ten tooth samples with at least one identified carious site on each of them were selected for the following trials. Figure 10 shows the X-ray images and photographs of two typical tooth samples. Before being tested, the tooth samples had been stored in thymolized physiological saline immediately after being extracted. The *in vitro* tests were performed as illustrated in Fig. 11, while the tooth samples were secured by locating their root tips into a thick layer of wax. For approximal caries detection experiment, pairs of teeth, which are: (1) both healthy, (2) one healthy and one carious, or (3) both carious on adjacent surfaces, were mounted closely as shown in Fig. 15. Air-flows from top, front, and back sides were employed to insulate the liquid from surrounding saliva, and to regulate its spreading. In order to simulate the conducting path across oral tissues, a thin layer of conducting gel (KY Jelly, Johnson & Johnson) was applied over the wax, in contact with the tooth roots. When used clinically, the second electrode could be either placed on the inner lip or held in the patient's hand (White et al. 1978). Meanwhile, normal saline solution (Otsuka Pharmaceuticals) was filled into the fluid tube, which is 500 μm in inner- diameter and made of silicone, and shaped into a column of 10 cm long. A 3-cm-long, highly viscous KY Jelly column was then applied on top of the saline solution. Afterward, the probe assembly was mounted on a three-axis stage, which was employed to maintain stable contact between the probe tip and a tooth sample when tested. As shown in Fig. 11, the measurement was performed by feeding sinusoidal potentials (with frequency ranging between 100 and 10,000 Hz supplied by a function generator) through the probe tip to a tooth sample, and collecting the resulted current signals for analysis. The applied potentials and resulting currents were maintained at relatively low levels (less than 2 V and 0.1 mA), while the currents for *in vivo* application might need to be maintained below the pain threshold (1 μA; Huysmans et al. 1996). To effectively capture these small electrical signals, a lock-in amplifier (SR810, Stanford Research Systems) was employed to intensify the current signals at specific measured frequency. At the end, histology was performed to validate the absence, presence, or extent of caries in the sample teeth. Tooth samples were sliced and ground into roughly 400 μm thick sections in a buccolingual direction, observed under a stereomicroscope, and classified using the criteria originally developed by Downer (Downer 1975).


**Fig. 10** X-ray images and photographs of selected sound and carious sites on two sample teeth

## 5 Results and discussion

Overall, *in vitro* caries detection trials on ten selected tooth samples (with one sound and one carious sites on each of them) were performed using the proposed fluidic probe. The impedance measurement of each site was repeated five times and the average and variation values measured at 1,000 Hz are listed in Table 1, which also show the histology results. Furthermore, Fig. 12 compares four sets of collected impedance values when various carious and sound sites (as indicated in Fig. 8) were investigated. The measured results may vary between tooth samples, while the typical impedance values of sound and carious teeth were around the magnitudes of MΩ and tens of kΩ, respectively. It was verified that the impedances measured across carious sites were at least 20 times lower than those across healthy ones, and the values also indicated the current stages of the developing dental caries. To account for the variations between teeth and patients, when applied clinically, the identification of caries must be based on the impedances actually measured on the patient's teeth. For example, the impedances across clearly identified sound and carious sites should be measured first to calibrate the detection process. In cases that solid tips were employed (by replacing the plastic probe head with a metal one whose diameter is 500 μm at its spherical tip), the measured impedances (as shown in Fig. 13) were usually higher, or even reached unexpectedly high values because of the excessive impedances probably caused by the rough and air-dried contacts. For example, the measured impedance across a carious site was close to that across a sound site, and both were two to three orders higher than the fluidic-

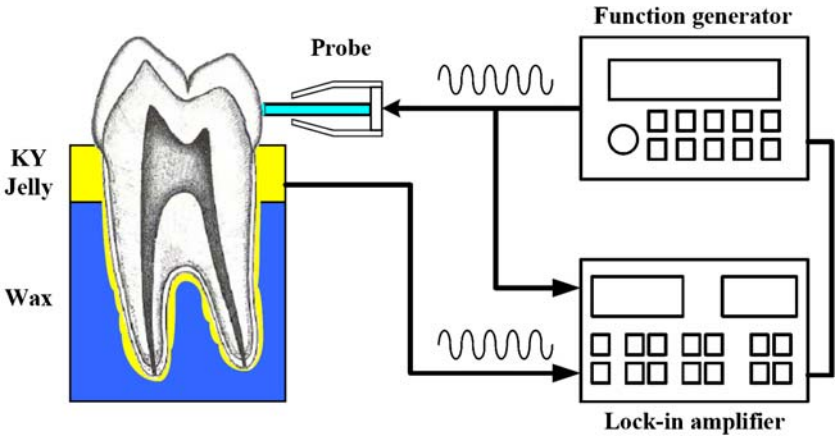


**Fig. 11** Experimental setup for the impedance measurement of tooth samples

probe measured values. With the high measured impedances, it would be very likely to incorrectly identify carious sites as sound ones. Meanwhile, the relatively low impedances measured using fluidic probes indicate that the liquid tips were capable of self-adapting their shape to teeth, which have varying and curved surfaces. On the other hand, the lack of shielding air-flow (by turning off the pressurized air supply) could potentially result in undesired low measured impedances as illustrated in Fig. 14. Since saliva is a good conducting media, it is possible that current would flow along the thin saliva films deposited on the tooth surface, rather than across the bodies of the tooth samples. For example, the measured impedances across sound sites were at least one order lower than the fluidic-probe measured values, and the ratio between impedances across sound and carious sites dropped from >50 to <5 in one case (N01). This might reduce the impedance differences and make it more difficult to distinguish caries teeth (especially these in their early stages) from healthy ones. As such, it is concluded that the proposed fluidic probe could function as a proper liquid bridge for current conduction and potential noise is limited by the surrounding air sleeve.

In additional to exposed caries, the presented fluidic probe could be modified and applied to the detection of approximal caries, which locates in the contacting surfaces of two adjacent teeth and is difficult to detect using most available schemes. Since the embrasures of contacting teeth are usually narrow and irregular in shape, it is difficult to build physical contact or transmit/receive signals to/from the caries sites within the embrasures. Based on the demonstrated self-adaptive and sensing mechanisms, the fluidic probe was further modified as shown in Fig. 15 in order to detect approximal caries. A liquid tip, which spontaneously spreads and fills the gaps, was used to explore the barely reachable carious sites between adjacent teeth, while surrounding three-dimensional air-flows were employed to insulate them from the environment. The ring-shaped flow guide was made of polydimethylsiloxane (PDMS) and fabricated by a molding process. Since approximal caries is usually very close to gingival papilla, it is likely that the liquid tip would mix with sulcus liquid and cause significant measurement errors. To avoid the potential connection between sulcus liquid and the liquid tip, a certain portion of air was ejected below the liquid tip,

**Table 1** Impedance measurement, average and variation values measured at 1,000 Hz at various carious sites

| Parameter | Carious site | | | | | | | | | |
|---|---|---|---|---|---|---|---|---|---|---|
| Electrical-impedances of 10 carious sites measured at 1 kHz (unit: kΩ) | | | | | | | | | | |
| Number | N01C | N02C | N03C | N04C | N05C | N06C | N07C | N08C | N09C | N10C |
| Average | 84.3 | 40.2 | 78.1 | 58.5 | 11.4 | 39.2 | 62.3 | 16.4 | 20.5 | 31.2 |
| Variation | 6.3% | 7.5% | 6.1% | 6.6% | 6.8% | 7.1% | 6.4% | 5.9% | 5.8% | 6.7% |
| Histology Result | Enamel caries | Dentin caries | Enamel caries | Enamel caries | Dentin caries | Dentin caries | Enamel caries | Dentin caries | Dentin caries | Enamel caries |
| Electrical-impedances of 10 sound sites measured at 1 kHz (unit: MΩ) | | | | | | | | | | |
| Number | N01S | N02S | N03S | N04S | N05S | N06S | N07S | N08S | N09S | N10S |
| Average | 3.84 | 1.98 | 2.43 | 2.23 | 1.72 | 4.57 | 3.95 | 2.19 | 2.84 | 2.61 |
| Variation | 8.6% | 7.9% | 10.2% | 9.4% | 8.5% | 8.1% | 9.2% | 8.8% | 9.0% | 8.8% |

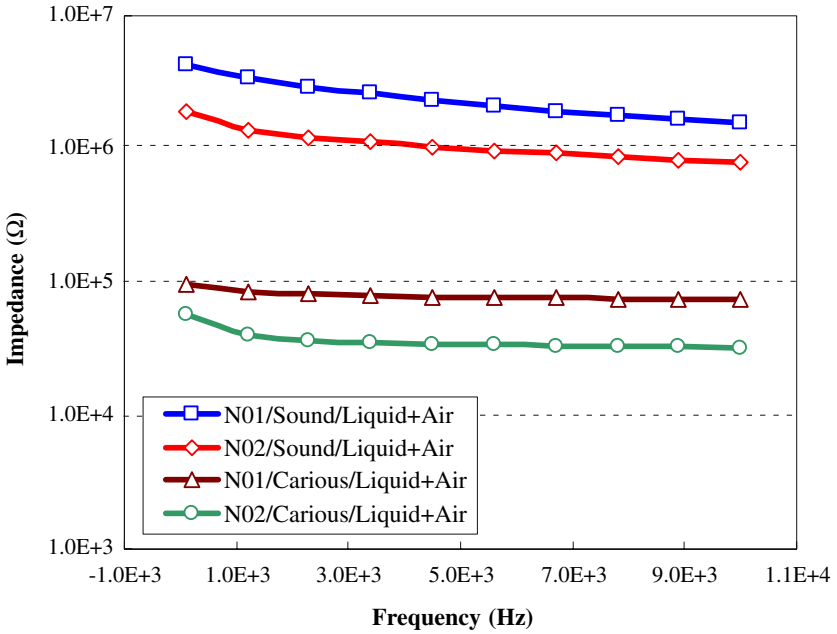


**Fig. 12** Measured impedances when both liquid tip and air sleeve were employed

from both front and back sides of the teeth. The air would expel the surrounding sulcus liquid and regulate the spreading of the liquid tip. In this scheme, the induced current flowed across both two teeth in parallel, and the resultant impedance was closer to that of the path with higher electrical conductivity. In our preliminary trials, ten cases (both healthy ×3, one healthy and one carious ×4, and both carious ×3) were performed and the measured results indicated that the impedances when at least one carious site appearing inside the gaps were around 0.08 MΩ (with a variation of 25.7%). Meanwhile, pairs of healthy teeth resulted in impedances of roughly 8 MΩ (with a variation of 16.2%), which were 100 times higher than those of carious teeth. The modified fluidic probe is promising in identifying approximal caries, which could be distinguished from healthy ones by its much lower impedance, while further design improvement and experimental verification are still required.

## 6 Conclusion

We have successfully demonstrated a miniature fluidic probe that is capable of self-adapting its shape to teeth and

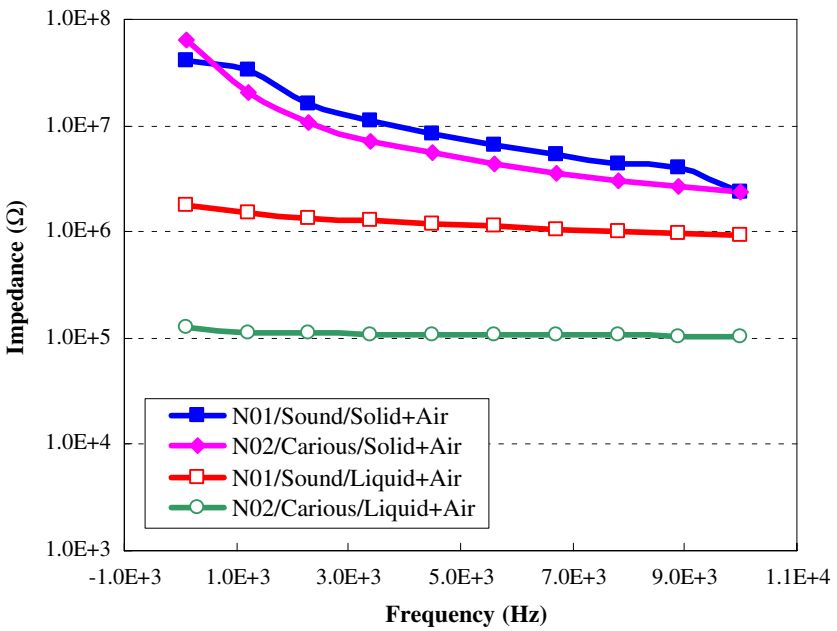


**Fig. 13** Measured impedances when liquid tips were selectively employed

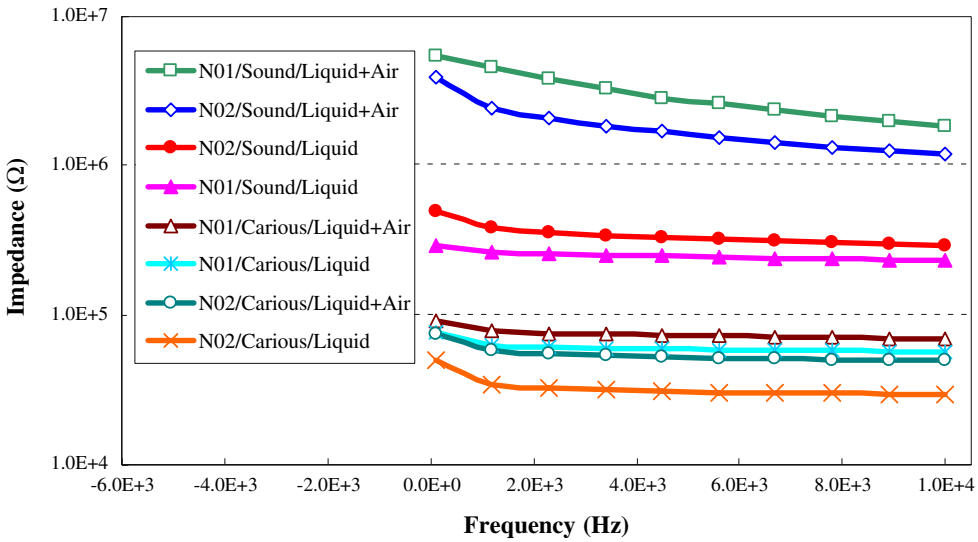


**Fig. 14** Measured impedances when air sleeves were selectively employed

cooperating with electrical devices to detect dental caries by sensing the variation in electrical-impedance. The fluidic probe, whose liquid tip spontaneously spreads on hydrophilic tooth surfaces and into underlying caries, is employed to create intimate electrical contact for impedance sensing. A tubular air sleeve shaped by the probe casing is applied around the liquid tip to insulate it from surrounding saliva, and to regulate its spreading. In addition, a friction damper that acts against gravity, air pressure, and surface tension is integrated to stabilize the actuation of fluidic probe. In the prototype demonstration, un-restored, extracted premolar teeth were investigated and the results indicated >20-fold impedance differences between sound and carious teeth, by which caries could be identified in a consistent manner. It is also verified that: (1) the employment of shielding air-flow eliminates the disruption from saliva, which can lower the measured impedances and mistakenly label sound teeth as carious ones, and (2) the application of liquid tips avoids the problem associated with rough contacts, which can raise the measured impedances and incorrectly identify carious teeth as sound ones. Furthermore, the fluidic probe has been applied to detect approximal caries, which hides between adjacent teeth and is barely detected by existing techniques. In this scheme, reliable electrical connection can be created to identify approximal caries, which is highly distinguishable by its much lower impedance compared to healthy teeth. As such, the proposed self-adaptive fluidic probe could readily serve as a diagnostic tool, which is critical to caries prevention and dental-care applications.

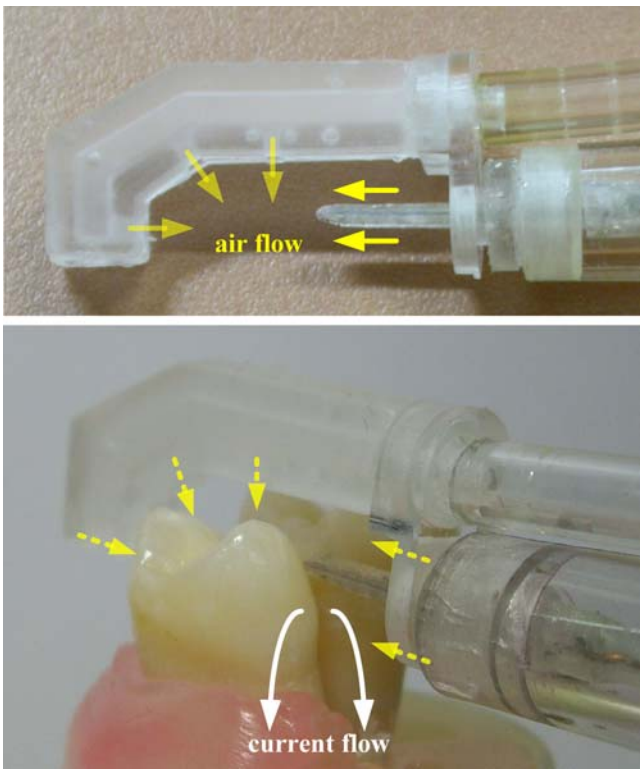


**Fig. 15** Modified fluidic probe and experimental setup for approximal caries detection

**Acknowledgements** The authors would like to express their appreciation to Dr. Pei-Chen Hu for help in preparing and examining tooth samples for caries detection trials. This work was supported in part by the National Science Council of Taiwan under Contract No. NSC 95-2221-E-007-226. The demonstrated systems were fabricated in the ESS Microfabrication Lab. at National Tsing Hua University, Taiwan.

## References


A.W. Adamson, A.P. Gast, *Physical Chemistry of Surfaces* (Wiley, New York, 1997)

P.F. Ashley, A.S. Blinkhorn, R.M. Davies, Occlusal caries diagnosis: An *in vitro* histological validation of the Electronic Caries Monitor (ECM) and other methods J. Dentistry **26**, 83–88 (1998)

E. Barsoukov, J.R. Macdonald, *Impedance Spectroscopy Theory, Experiment, and Applications* (Wiley-Interscience, Hoboken, 2005)

H.C. Benedict, The fluorescence of teeth as another method of attack on the problem of dental caries J. Dent. Res. **9**, 274–275 (1929)

M. Culjat, R.S. Singh, D.C. Yoon, E.R. Brown, Imaging of human tooth enamel using ultrasound IEEE T. Med. Imaging **22**, 526–529 (2003)

M.C. Downer, Concurrent validity of an epidemiological diagnostic system for caries with the histological appearance of extracted teeth as validating criterion Caries Res. **9**, 231–246 (1975)

R. Hibst, R. Gall, Development of a diode laser based fluorescence caries detector Caries Res. **32**, 294 (1998)

M.C. Huysmans, C. Longbottom, N.B. Pitts, P. Los, P.G. Bruce, Impedance spectroscopy of teeth with and without approximal caries lesions—an *in vitro* study J. Dent. Res. **75**, 1871–1878 (1996)

S. Keem, M. Elbaum, Wavelet representations for monitoring changes in teeth imaged with digital imaging fiber-optic transillumination IEEE T. Med. Imaging **16**, 653–663 (1997)

M. Kumasaki, An electric characteristic of the tooth and its equivalent circuit, part 1 J. Osaka Dent. Univ. **9**, 9–18 (1975)

S. Lees, F.E. Barber, Looking into teeth with ultrasound Science **161**, 477–478 (1968)

M. Levinkind, T.J. Vandernoot, J.C. Elliott, Electrochemical impedance characterization of human and bovine enamel J Dent Res **69**, 1806–1811 (1990)

C. Longbottom, M.C. Huysmans, Electrical measurements for use in caries clinical trials J. Dent. Res. **83**, C76–C79 (2004)

C. Longbottom, N.B. Pitts, B. Lawrenson, Electronic diagnosis of approximal caries utilizing a metal-coated plastic strip/wedge Caries Res. **27**, 207 (1993)

C. Longbottom, M.C. Huysmans, N.B. Pitts, P. Los, P.G. Bruce, Detection of dental decay and its extent using AC impedance spectroscopy Nat. Med. **2**, 235–237 (1996)

J.M. Mumford, Relationship between the electrical resistance of human teeth and the presence and extent of dental caries Br. Dent. J. **100**, 239–244 (1956)

P.E. Peterson, *The World Oral Health Report 2003: Continuous Improvement of Oral Health in the 21st Century – the Approach of the WHO Global Oral Health Programme* (World Health Organization, Geneva, 2003)

I.A. Pretty, Caries detection and diagnosis: Novel technologies J. Dentistry **34**, 727–739 (2006)

R.H. Selwitz, A.I. Ismail, N.B. Pitts, Dental caries Lancet **369**, 51–59 (2007)

C.M. Sturdevant, R.E. Barton, C.L. Sockwell, W.D. Strickland, *The Art and Science of Operative Dentistry* (The C. V. Mosby Company, St. Louis, 1985)

F. Sundström, K. Fredriksson, S. Montan, U. Hafström-Björkman, J. Ström, Laser-induced fluorescence from sound and carious tooth substance: spectroscopic studies Swed. Dent. J. **9**, 71–80 (1985)

S. Tranæus, X.Q. Shi, B. Angmar-Mansson, Caries risk assessment: methods available to clinicians for caries detection Community Dent. Oral. **33**, 265–273 (2005)

G.E. White, A. Tsamtsouris, D.L. Williams, Early detection of occlusal caries by measuring the electrical resistance of the tooth J. Dent. Res. **57**, 195–200 (1978)